GLOBAL BIOGEOCHEMICAL CYCLES, VOL. 24, GB1001, doi:10.1029/2008GB003336, 2010

Click Here for Full Article

Nitrogen cycling and feedbacks in a global dynamic land model

Stefan Gerber,[1] Lars O. Hedin,[1] Michael Oppenheimer,[2,3] Stephen W. Pacala,[1] and Elena Shevliakova[1]

Received 20 August 2008; revised 17 July 2009; accepted 11 August 2009; published 1 January 2010.

[1] Global anthropogenic changes in carbon (C) and nitrogen (N) cycles call for modeling tools that are able to address and quantify essential interactions between N, C, and climate in terrestrial ecosystems. Here we introduce a prognostic N cycle within the Princeton–Geophysical Fluid Dynamic Laboratory (GFDL) LM3V land model. The model captures mechanisms essential for N cycling and their feedbacks on C cycling: N limitation of plant productivity, the N dependence of C decomposition and stabilization in soils, removal of available N by competing sinks, ecosystem losses that include dissolved organic and volatile N, and ecosystem inputs through biological N fixation. Our model captures many essential characteristics of C-N interactions and is capable of broadly recreating spatial and temporal variations in N and C dynamics. The introduced N dynamics improve the model's short-term NPP response to step changes in CO_2. Consistent with theories of successional dynamics, we find that physical disturbance induces strong C-N feedbacks, caused by intermittent N loss and subsequent N limitation. In contrast, C-N interactions are weak when the coupled model system approaches equilibrium. Thus, at steady state, many simulated features of the carbon cycle, such as primary productivity and carbon inventories, are similar to simulations that do not include C-N feedbacks.

Citation: Gerber, S., L. O. Hedin, M. Oppenheimer, S. W. Pacala, and E. Shevliakova (2010), Nitrogen cycling and feedbacks in a global dynamic land model, *Global Biogeochem. Cycles*, *24*, GB1001, doi:10.1029/2008GB003336.

1. Introduction

[2] The terrestrial vegetation is a critical player in the dynamics of the Earth system. A number of biophysical and biogeochemical interactions couple the land surface to the atmosphere's radiative balance, circulation, and chemical composition; moreover, the terrestrial biosphere is an integral part of global biogeochemical cycling [*Foley et al.*, 2003]. Global cycles of carbon (C) and nitrogen (N) are increasingly altered by human dependence on fossil C for energy, artificial fertilizer for food production, and disturbance of landscapes for development [*Pacala et al.*, 2001; *Galloway et al.*, 2004; *IPCC*, 2007]. Identification, understanding, and prediction of these human impacts represent some of our most urgent scientific challenges.

[3] Uncertainties in the quantification of feedbacks between the terrestrial and the larger Earth system are considerable and have important consequences for projections of climate change over the next century [*Cox et al.*, 2000; *Friedlingstein et al.*, 2006]. For example, terrestrial C cycle models predict that increased atmospheric CO_2 should stimulate plant CO_2 uptake and thus lead to increased burial and storage of C in terrestrial ecosystems [*Cramer et al.*, 2001; *Gerber et al.*, 2004] and thereby dampen the climate effects of anthropogenic CO_2 emissions [*Joos et al.*, 2001]. A major problem with this so-called "CO_2 fertilization" is that the models used do not consider the effects of nutrient availability which may be insufficient to support the plant and soil C sinks [*Oren et al.*, 2001; *Hungate et al.*, 2003].

[4] A second phenomenon of concern is the anthropogenic inputs of biologically available N into terrestrial landscapes [*Galloway et al.*, 2004] in form of artificial fertilizer, through cultivation of N fixing crops, and via fossil fuel burning. Overall, these N fluxes are thought to have doubled since the late 19th century, causing "N saturation" or the accumulation of excess N in some terrestrial systems. These complex interactions between climate, C, and nutrients call for a new generation of models that can explicitly handle the interaction of climate and biogeochemistry.

[5] Terrestrial components of modern Earth System Models (ESMs) link ecosystem-scale cycles of water and C, simulate changes in the biogeographical distribution of plant functional types [e.g., *Kucharik et al.*, 2000; *Sitch et al.*, 2003], and couple global biogeochemical cycles with the general circulation of atmosphere and ocean [*Cox et al.*, 2000; *Friedlingstein et al.*, 2006; *Shevliakova et al.*, 2009].

[1]Department of Ecology and Evolutionary Biology, Princeton University, Princeton, New Jersey, USA.
[2]Woodrow Wilson School of Public and International Affairs, Princeton University, Princeton, New Jersey, USA.
[3]Department of Geosciences, Princeton University, Princeton, New Jersey, USA.

Copyright 2010 by the American Geophysical Union.
0886-6236/10/2008GB003336$12.00

While N dynamics are considered in some terrestrial models, the treatment of key processes and feedbacks has been rather limited, and further development is urgently needed. In this class of models, the most complete treatment is presently found in CLM-CN [*Thornton et al.*, 2007]. It tracks aboveground and belowground N pools, allows for N limitation on photosynthesis, and simulates inorganic N losses. Other models have incorporated parts of N cycling: IBIS [*Kucharik et al.*, 2000] simulates storage of N in vegetation and soils, export of N via denitrification, and inorganic leaching, but it does not treat plant N uptake or plant-soil feedbacks dynamically.

[6] In a different approach from ESMs, "biogeochemical models" have been developed to explicitly treat interactions between C and growth-limiting nutrients (mainly N and phosphorus) in terrestrial ecosystems. CENTURY [*Parton et al.*, 1987, 1993, 1994] is widely used; particularly, its decomposition module has been adopted by several models. TEM [*Raich et al.*, 1991] accounts for interactions between C and N by changing allocation efforts depending on C and N demands. In MEL [*Rastetter et al.*, 1997] an acclimation also adjusts C and N uptake to maintain a specific C:N ratio; subsequent developments account for N fixation on the basis of resource optimization [*Rastetter et al.*, 2001] and DON losses [*Rastetter et al.*, 2005]. These models have significantly helped to improve our understanding of the terrestrial element cycle and are an important basis to develop comprehensive terrestrial components of ESMs [*Thornton et al.*, 2007; *Xu-Ri and Prentice*, 2008]. However, because these biogeochemical models are often parameterized on the basis of specific locations, often do not resolve diurnal scales of water and energy exchange between land and atmosphere, and do not simulate changes in vegetation distribution and structure, they are not suitable as ESM components.

[7] Here we introduce the core of an interactive terrestrial C-N model that can be incorporated in an ESM framework and that couples biophysical and a biogeochemical (i.e., C and N) dynamics. We outline the most essential processes required to capture key dynamics and feedbacks of the plant-soil-climate system and describe how we resolve these requirements in the model. We then analyze the coupled C-N dynamics at steady state and examine the model's response to physical disturbance and to a step change in atmospheric CO_2. Finally, we investigate the role of the key feedbacks in sensitivity experiments.

2. Model Structure and Approach

2.1. LM3V Land Model

[8] We added a prognostic N cycle to the LM3V dynamic vegetation model developed at Princeton University and the Geophysical Fluid Dynamics Laboratory (GFDL) [*Shevliakova et al.*, 2009]. LM3V is the interactive land component of the GFDL ESM2.1 which captures vegetation, C, and water dynamics. The land-surface component of LM3V simulates land-atmosphere exchange of heat, water, and momentum. The biophysical component calculates photosynthesis on the basis of stomatal conductance using a form of the Farquhar scheme [*Farquhar et al.*, 1980] and further developments [*Collatz et al.*, 1991, 1992]. The biogeography component simulates distribution of five plant functional types (PFTs): C3 grasses, C4 grasses, tropical forest trees, temperate deciduous trees, and temperate evergreen trees. A tile (a subgrid fraction consisting of primary, crop, pasture, and various levels of secondary vegetation; see *Shevliakova et al.* [2009] for the exact definition) is occupied by a single PFT. Each PFT has five C pools representing leaves, fine roots, sapwood, labile, and heartwood pools. LM3V explicitly treats fire frequency as a dynamical property of soil dryness, fuel load, and tissue-specific fire resistance.

[9] We maintain the basic structure of LM3V and pair each C pool in vegetation and soil with a respective N compartment, but extend the LM3V decomposition model by two additional belowground pools. Several essential processes and feedbacks couple vegetation dynamics with the N cycle which we address in detail in this paper (Figure 1). First, we include N limitation on plant growth and CO_2 assimilation. Second, we develop a soil N feedback which explicitly allows inorganic forms of N to influence soil C and N mineralization, and the formation of recalcitrant "stabilized" soil organic matter. Third, we resolve the competing processes that determine the balance of available N in soils, including plant uptake, sorption, microbial/soil immobilization, and export via hydrological or gaseous losses. Fourth, we allow vectors of organic N losses that circumvent mechanisms of biotic retention and are therefore critical for the development of terrestrial N limitation: leaching of dissolved organic N (DON) and volatile N escape during fire. Fifth, we model biological N fixation (BNF) as a function of N availability, coupled with an energetic cost and the presence of N fixing tree species. In the following sections we address the key ecological and biogeochemical processes that define each of these components and present the basic model structure and formulation that capture these processes. The equations of state for different carbon and nitrogen compartments are summarized in Text S1.[1]

2.2. Coupling Carbon and Nitrogen in Plants

[10] The essential role of N in photosynthesis is relatively well understood. N is highly concentrated in Rubisco, the enzyme that catalyzes the assimilation of atmospheric CO_2 [*Field and Mooney*, 1986]. However, a simple measure of plant N status and its feedback on productivity remains elusive, in part because the physiological use of N in plants varies across and within species (e.g., photosynthesis, herbivory defense, structure, storage, etc.).

[11] We therefore use a simple Liebig's law of the minimum approach to model plant level C-N feedbacks where plants adjust their uptake of C and N to maintain a specific stoichiometry in tissues, similar to other biogeochemical models [*Raich et al.*, 1991; *Rastetter et al.*, 1997; *Schimel et al.*, 1997]. While PFT-specific C:N ratios of tissues remain constant, we define an additional storage pool (S) to which N is allocated once the N requirements for

[1]Auxiliary materials are available in the HTML. doi:10.1029/2008GB003336.

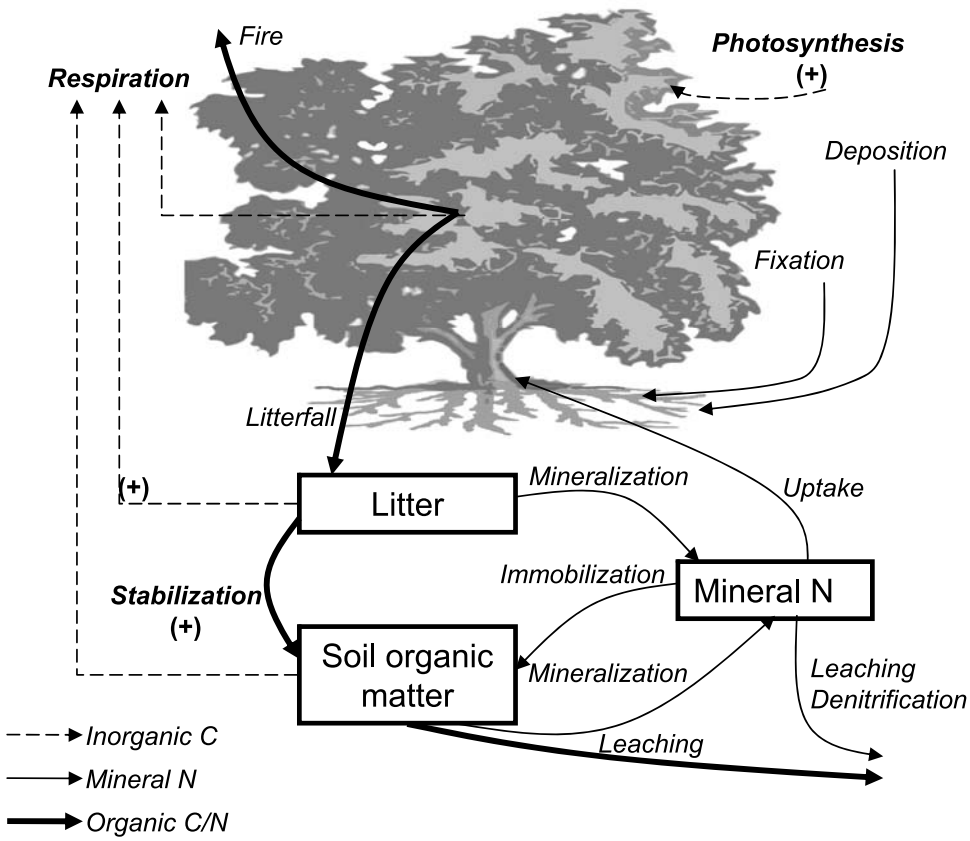

Figure 1. Schematics of the terrestrial C-N model. The arrows depict the fluxes of inorganic C (dashed), mineral N (thin solid), or organically bound C and N (thick solid) with the associated processes (italic). Processes highlighted in bold face denote instances where N availability positively (plus signs) affects carbon cycling rates.

tissues are satisfied. Total N in the vegetation (N_{veg}) is therefore

$$N_{\mathrm{veg}} = \frac{C_w}{r_w} + C_{\mathrm{liv}}\left(\frac{p_l}{r_l} + \frac{p_r}{r_r} + \frac{p_{\mathrm{sw}}}{r_{\mathrm{sw}}} + \frac{p_{\mathrm{vl}}}{r_{\mathrm{vl}}}\right) + S \qquad (1)$$

where C_w is the C in heartwood; C_{liv} is the C in living tissues leaves, roots, labile, and sapwood; p_l, p_r, p_{vl}, and p_{sw} are the partitioning fractions of C among the living pools (leaves, roots, labile, and sapwood, respectively); and r_w, r_l, r_r, r_{vl}, and r_{sw} denote the PFT-specific C:N ratio of the respective tissues (see Table S1 and Text S1 for the detailed allocation scheme and a list and values of parameters).

[12] Retranslocation of N occurs before leaf abscission in deciduous PFTs [*McGroddy et al.*, 2004], but not during fine root loss [*Gordon and Jackson*, 2000]. Losses from tissue turnover $Q_{N,\mathrm{liv}}$ are therefore

$$Q_{N,\mathrm{liv}} = C_{\mathrm{liv}}\left(\frac{\alpha_l p_l (1 - l_f)}{r_l} + \frac{\alpha_r p_r}{r_r} + \frac{\gamma p_{\mathrm{sw}}}{r_w}\right) \qquad (2)$$

where α_l and α_r the tissue-specific turnover rate of leaves and roots, respectively; γ is the conversion rate of sapwood into heartwood; and l_f is the fraction of leaf N retranslocated. Herbivory losses are implicitly treated as part of the plant's tissue turnover, although plant-herbivory interactions may change with N availability [*Throop et al.*, 2004].

[13] Instead of prescribing ranges of C:N ratios in the different tissues, we buffer N in plants via storage (S). Diurnal and seasonal cycles generate asynchronies in element assimilation and thus temporary imbalances in stoichiometry. These asynchronies affect the variability in plant stoichiometry the more the faster tissues turn over. It is a reasonable assumption that plants are fitted to buffer the relatively predictable intra-annual fluctuations in nutrient supply versus demand [*Chapin et al.*, 1990]. If nutrient supply is sufficient, we allow plants to accumulate N to storage up to 1 year worth of tissue turnover:

$$S_{\mathrm{target}} = t_h Q_{N,\mathrm{liv}} \qquad (3)$$

where S_{target} is the optimum storage size realized under sufficient nutrient supply and t_h is the planning horizon (t_h = 1 year), the time over which plant losses are buffered. This concept avoids short-term switches between N sufficiency and N limitation in plants and is independent of PFT-specific C:N ratio and rate of tissue regeneration. In turn, we define plant N status (x) at a given time as the fraction of the actual N

reserve compared to the target storage size: $x = S/S_{\text{target}}$. N regulation of photosynthesis and soil N uptake operate as a function of plant N status:

$$A_{g,N} = A_{g,\text{pot}}(1 - e^{-x\varphi}) \tag{4}$$

$$U_{N,P} = U_{N,P,\text{pot}} * \begin{cases} 1 & x < 1 \\ 0 & \text{else} \end{cases} \tag{5}$$

where $A_{g,N}$ is the N limited gross photosynthesis and $A_{g,\text{pot}}$ is the potential photosynthesis under sufficient N supply (i.e., not N limited), while φ is a parameter that allows for metabolic deficiencies as plant N contents decrease. Downregulation of photosynthesis reduces stomatal conductance and, subsequently, transpiration and latent heat fluxes [*Collatz et al.*, 1991, 1992; *Burns et al.*, 2001]. Plant N uptake ($U_{N,P}$) from the soil-available pool (NH_4^+, NO_3^-) proceeds at the potential rate $U_{N,P,\text{pot}}$ (see equation (10)) as long as N in storage is below the target size (equation (3)).

2.3. Soil Carbon-Nitrogen Feedbacks and Mineralization of Organic Matter

[14] The decomposition of plant litter by heterotrophic microbes ultimately causes the mineralization of organically bound C and nutrients; i.e., the release into forms available for plant uptake (e.g., NO_3^- or CO_2). Organic matter decomposition is strongly influenced by the abiotic factors of soil temperature, moisture [*Lloyd and Taylor*, 1994; *Foley*, 1995], and physical soil characteristics such as porosity and mineral composition [*Oades*, 1988]. Decomposition models such as CENTURY therefore traditionally use a suite of discrete pools feeding into each other, each with a characteristic turnover time [*Parton et al.*, 1987; *Bolker et al.*, 1998]. Below, we discuss models of microbial N limitation, address theory and evidence how available N influences decomposition and stabilization of litter and soil carbon, and introduce a decomposition module that is a modified form of the CENTURY approach.

[15] The narrow C:N ratio of soil microbes compared to plant litter stoichiometry is argued to be a limiting factor during decomposition: to sustain microbial growth, the amount of N supplied per unit C consumed is too little. Rates of decomposition vary with substrate C:N ratio [*Melillo et al.*, 1982] but can also be stimulated by N additions [e.g., *Downs et al.*, 1996]. However, the stimulating effect of N is not always seen, and often N seems to inhibit respiration (see review by *Fog* [1988] and, more recently, *Knorr et al.* [2005]). Long-term fertilization experiments show that N additions possibly trigger two processes that have opposite effects on respiration signals [*Neff et al.*, 2002; *Li et al.*, 2006]: First the "light" fraction of soil organic matter that is often chemically and visually similar to litter [*Swanston et al.*, 2004] decreases in the fertilized plots, indicating that N additions stimulate its decomposition. Second, the amount of "heavy" soil organic matter that consists of organic material adsorbed to mineral surfaces or organo-mineral macroaggregates [*Sollins et al.*, 1984] increases following fertilization. Overall, these observations suggest the existence of two competing mechanisms where on the one hand N stimulates the transformation of "light" plant litter, but on the other hand N acts to stabilize carbon in "heavy" soil organic matter.

[16] While it seems intuitive that differences in C:N ratio between substrate and decomposers causes N limitation in microbes, it is at the same time challenging to set up a modeling framework where N-dependent decomposition is sustained. In primitive models of microbial dynamics, microbial mass grows indefinitely when only restricted by N availability (see Text S2): A high N-immobilization capacity of microbes results in a quick buildup of microbial biomass that is accelerated by N supplied from litter consumption and in turn would further enhance rates of decomposition and microbial growth. This explosion can be slowed down, if microbial N waste is not immediately mineralized, but is instead trapped in secondary organic materials. Yet over time, as the secondary materials decay, the previously trapped N becomes available again. Therefore N limited decomposition would occur only transiently. Indeed, in most biogeochemical models, N limitation is not maintained, but appears only after events of vegetation disturbance that drastically increase the amount of N-poor litter; but decomposition rates return quickly to levels dictated by C availability.

[17] In Text S2, we present a theoretical framework that leads to sustained microbial N limitation during decomposition of litter with high C:N ratio: This particular concept requires restricted access to C due to a finite litter surface area. It follows that mineralization of C and N is a linear combination of the supply of available N to microbes dwelling on litter surfaces and their respiration rate (see Text S2 for a complete derivation). In such a case the decomposition rate has the general form

$$F_L = kL(1 + \xi[N_{\text{av}}]) \tag{6}$$

where F_L is the rate at which the litter is processed, k is a first-order decomposition rate, L is the size of the litter pool, $[N_{\text{av}}]$ is the concentration of available mineral N (NO_3^-, NH_4^+) in soils, and ξ is a parameter. Although we pointed out one particular process that leads to equation (6), this formulation may also be thought of as a first-order Taylor approximation of a general function $F_L([N_{\text{av}}])$ from any mechanism that leads to a response of decomposition to N additions. Most generally, parameters in equation (6) pool properties that affect litter degradation, such as substrate quality, C:N ratio of litter and microbes, litter surface/volume ratio, microbial N uptake rates, trade-offs among microbial communities, etc.

[18] Negative effects of available N on carbon release in soils have so far not been considered in global models. Here we explicitly allow for N_{av} to influence carbon residency time by increasing C and N fluxes into the recalcitrant pool reflecting the increasing amount of stabilized (heavy) materials occurring in fertilization experiments:

$$q = \frac{q_{\max}[N_{\text{av}}]}{k_{s,1/2} + [N_{\text{av}}]} \tag{7}$$

Table 1. Input, Linear Transfer, and Decomposition Matrix of C and N in the Soil Module[a]

	LF	LS	SS	SP	Litterfall (Q_L)
			Carbon		
LF	$-Ak_{\mathrm{LF}}$	0	0	0	$\max(a_{\mathrm{LF}} - b_{\mathrm{LF}} f_{\mathrm{lig}} r_T, f_{\mathrm{LF,min}})$
LS	0	$-Ak_{\mathrm{LS}}\,(1 + \xi[N_{\mathrm{av}}])$	0	0	$1 - \max(a_{\mathrm{LF}} - b_{\mathrm{LF}} f_{\mathrm{lig}} r_T, f_{\mathrm{LF,min}})$
SS	0	$Ak_{\mathrm{LS}}\,(1 + \xi[N_{\mathrm{av}}])\frac{q_{\max}[N_{\mathrm{av}}]}{k_{S,1/2}+[N_{\mathrm{av}}]}$	$-Ak_{SS}$	0	0
SP	0	$Ak_{\mathrm{LS}}\,(1 + \xi[N_{\mathrm{av}}])q_{\mathrm{SP}}$	0	$-Ak_{\mathrm{SP}}$	0
			Nitrogen		
	LF	LS	SS	SP	Litterfall ($Q_{\mathrm{L,N}}$)/Transfers into SS/SP
LF	$-Ak_{\mathrm{LF}}$	0	0	0	$\min\left(\frac{r_T}{r_{\mathrm{LS,min}}}, 1\right)\max(a_{\mathrm{LF}} - b_{\mathrm{LF}} f_{\mathrm{lig}} r_T, f_{\mathrm{LF,min}})$
LS	0	$-Ak_{\mathrm{LS}}\,(1 + \xi[N_{\mathrm{av}}])$	0	0	$1 - \left[\min\left(\frac{r_T}{r_{\mathrm{LS,min}}}, 1\right)\max\left(a_{\mathrm{LF}} - b_{\mathrm{LF}} f_{\mathrm{lig}} r_T, f_{\mathrm{LF,min}}\right)\right]$
SS	0	0	$-Ak_{\mathrm{SS}}$	0	$\frac{Q_{\mathrm{C,LS->SS}}}{r_{\mathrm{SS}}}$
SP	0	0	0	$-Ak_{\mathrm{SP}}$	$\frac{Q_{\mathrm{C,LS->SP}}}{r_{\mathrm{SP}}}$

[a]The rate of change of C and N in a particular pool in row 1 to 4 is the product of the row's matrix entries times the pool size (or litterfall) in the corresponding column. Note that the N transfer into soil pools SS and SP is an exception and is not multiplied with the column head. Instead these N transfers are linked to the respective carbon fluxes from LS to the SS and SP pools ($Q_{\mathrm{LS->SS}}$ and $Q_{\mathrm{LS->SP}}$) via fixed C:N ratio (r_{SS} and r_{SP}), requiring N immobilization. The diagonal elements represent decomposition with k_{LF}, k_{LS}, k_{SS}, and k_{SP} as the first-order decomposition constant for each pool, A is the combined soil temperature and soil moisture modifier, ξ, $q_{\max}$, $k_{S,1/2}$, are parameters that feed into C-N feedbacks during decomposition of LS and formation of SS (see equations (6) and (7)), $[N_{\mathrm{av}}]$ is the concentration of available N in the soil, and q_{SP} is the constant fraction of carbon decomposed in LS that is transferred to SP. External fluxes into the four pools are from C and N in litterfall ($Q_{\mathrm{L,C}}$, and $Q_{\mathrm{L,N}}$) which is partitioned on the basis of lignin to N ratio in the litter: r_T is the C:N ratio of the tissue in litterfall, f_{lig} is the fraction of lignin in litterfall, and a_{LF}, b_{LF}, and $f_{\mathrm{LF,min}}$ are parameters. C:N ratio in the slow litter is the minimum of r_T and a parameter $r_{\mathrm{LS,min}}$, while the rest of N in litterfall is transferred to LF.

where q is the fraction of litter stabilized, $q_{\max}$ is the maximum fraction stabilized, and $k_{s,1/2}$ is the half-saturation constant (i.e., the concentration at which $q = q_{\max}/2$).

[19] We replaced the two-soil-pool model by *Shevliakova et al.* [2009] with a four-pool structure based on CENTURY (Table 1). We define four functionally distinct soil pools that differ in turnover time and reflect resistance to transformation and decomposition: a fast versus slow litter pool (LF and LS) and a slow versus passive soil organic matter pool (SS and SP). Plant litterfall and root turnover is partitioned among LF and LS, depending on litter quality (Table 1); these compartments reflect primary "light" material. SS and SP turn over on time scales of decades and centuries, respectively. The decay rate of each of these litter and soil pools is modified by soil temperature and soil moisture on the basis of standard biophysical relationships [*Shevliakova et al.*, 2009]. Compared to CENTURY, both the number of pools and nondiagonal entries in the decomposition matrix have been reduced [*Bolker et al.*, 1998]. We introduce the C-N feedbacks (equations (6) and (7)) to occur during decomposition of the LS and the formation of SS (Table 1). LS collects resistant plant material and precursors of secondary soil organic matter, both of which appear to be most vulnerable to changes in N supply. In LF, N-stimulation of decomposition rates is conceivable, but its effect would be small as its share of the overall soil carbon and N inventory is marginal. The parameterization of the C-N feedbacks in equations (6) and (7) is based on recent experiments by *Li et al.* [2006]. We note that evaluating N effects on decomposition is an area of active research and that further validation is necessary to quantify belowground C-N interactions. However, the setup allows for great flexibility to explore uncertainties, and appropriate choices (e.g., $\xi = 0$ and big $k_{1,2}$ in equations (6) and (7)) easily allow to return to traditional models.

[20] The release of C (heterotrophic respiration, R_h) and N (mineralization) is the sum of all fluxes of material out of each pool minus the stabilization flux from LS into SS and SP. We assume that decomposers quickly approach a steady state because of the fast turnover rates and do not explicitly model microbial dynamics. Hence the microbial pool (m) is a purely diagnostic variable that can be calculated on the basis of respiration rate:

$$m = \frac{R_h}{\lambda_m e} \tag{8}$$

where λ_m is the microbial turnover and e is the efficiency (i.e., the proportion of respiration to overall turnover).

2.4. Competing Processes for Available Nitrogen

[21] Soil mineral N in form of ammonium and nitrate (available N) provides the overwhelming source of N for plant growth and microbe-soil organic matter interactions. We consider here four possible sinks of mineral N: sorption to soil particles, plant uptake, immobilization into long-lived organic compounds (slow and passive soil organic matter) via microbial or abiotic pathways, and hydrological leaching.

[22] We consider sorption/desorption as a fast process in the soil and allow this process to be at steady state in every time step, effectively operating as a buffer of available N (i.e., it does not alter the competition of the different sinks below but merely reduces all removal rates by the same factor):

$$N_{i,\mathrm{av}} = \frac{N_i}{b_{N,i}} \tag{9}$$

where the subscript i refers to either ammonium and nitrate and $b_{N,i}$ are buffer parameters [*Matschonat and Matzner*,

1995]. While N sorption depends on several factors that vary locally (e.g., pH or clay content), for simplicity we here consider the buffer factor to be globally constant.

[23] Plant assimilation is a combination of active and passive uptake of mineral N across the root surface: The active uptake follows a traditional Monod function, while passive transport is a linear function of available N and the plant transpiration flux [*Raich et al.*, 1991; *Rastetter et al.*, 1997]:

$$U_{N,P,\mathrm{pot},i} = \frac{\nu_{\max} C_r N_{i,\mathrm{av}}}{h_s\left(k_{p,1/2} + [N_{\mathrm{av}}]\right)} + \left[N_{i,\mathrm{av}}\right] Q_{W,T} \tag{10}$$

where $\nu_{\max}$ (yr^{-1} kgC^{-1}) is the maximum uptake rate per unit root mass C_r, $k_{p,1/2}$ is the half-saturation constant, $Q_{W,T}$ is the transpiration flux of water, and $[N_{\mathrm{av}}]$ is the concentration of the combined available mineral N pool (i.e., ammonium and nitrate, $[N_{\mathrm{av}}] = [N_{\mathrm{NH4,av}}] + [N_{\mathrm{NO3,av}}]$). The total N uptake rate at small concentrations $\sim \nu_{\max}/k_{p1/2} \times [N_{\mathrm{av}}]$ is assumed to be limited by diffusion of available N in soils [*Leadley et al.*, 1997]. Equation (10) also requires information on soil depth to convert available mineral N inventories into soil concentrations ($h_s[N_{i,\mathrm{av}}] = N_{i,\mathrm{av}}$). We approximate soil depth based on soil C assuming 3.4% C weight content and average soil density of 1500 kg m^{-3}.

[24] N immobilization into soil organic matter via abiotic and microbial pathways is extremely efficient [e.g., *Perakis and Hedin*, 2001]; we allow this process to have priority over plant N uptake and other sinks. N immobilization occurs during transfers from LS to SS and SP (Table 1 and equation (7)).

[25] Hydrological losses of available N are calculated based on drainage rate ($Q_{W,D}$):

$$L_i = Q_{W,D}\left[N_{i,\mathrm{av}}\right] \tag{11}$$

Nitrification that allows the partitioning between ammonium and nitrate is a linear function of ammonium concentrations, using the same temperature and moisture modifier as for the decomposition of soil organic matter (Table 1). We do not differentiate denitrification from NO_3^- leaching: Both NO_3^- leaching and denitrification are highest in N-rich conditions (when soil NO_3^- accumulates) and thus differ little in their functional influence on C-N feedbacks. Denitrification can in the future be explicitly considered by a first-order loss mechanism relative to soil NO_3^- that includes effects by moisture and other soil conditions.

[26] Allowing for competition for mineral N is critical to model long-term N dynamics: Its partitioning among different sinks affects N availability and therefore ecosystem functioning over time scales ranging from hours to days (sorption, microbes) over annual to multiannual (plants) up to several decades or millennia (soil sinks and losses). The desired order of preference for available N is sorption > soil immobilization > plant uptake > hydrology. This hierarchy can be achieved with sensible parameter choices (Table S1 and Text S1) asserting that $q_{\max}/k_{s,1/2}\,\mathrm{LS}/r_{\mathrm{SS}} > \nu_{\max}\, C_r/k_{p,1/2} > Q_D$ (see equations (7), (10), and (11) and Table 1).

2.5. N Losses From Organic Pools

[27] N losses that circumvent the plant-available pool of mineral N (i.e., soil NH_4^+ and NO_3^-) can be critical in determining the long-term C and N budget and dynamics in terrestrial ecosystems [*Hedin et al.*, 1995; *Perakis and Hedin*, 2002]. We allow for two such loss pathways: volatile N losses by fire and leaching losses of dissolved organic N (DON) to stream and groundwaters.

[28] Results from laboratory experiments suggest that 2 to 46 percent of biomass N remains in ashes after burning, compared to 1 to 22 percent of C [*Levine*, 1994; see *Delmas et al.*, 1995]. A comparison of C and N emissions based on the global fire emission data set [*van der Werf et al.*, 2006; *Randerson et al.*, 2007] suggests that up to 80% of the N is retained in the system. Given these inherent uncertainties, we approximate N volatilized as the C emissions from fire times the stoichiometric ratio of the burned tissues, reduced simply by global a retention factor that accounts for increased N concentrations in ash. Here, we set the retained fraction to 0.45, which is at the upper end of laboratory emission, but still below our estimations based on the global fire emission data set.

[29] A second loss vector that bypasses the available N pool is the hydrological export of dissolved organic N (DON): the N component of dissolved organic matter (DOM). Formation of DOM is believed to be associated with microbial decomposition of litter and soil organic matter [*Brooks et al.*, 1999]. DOM decomposition [*Qualls and Haines*, 1992] and chemical sorption [*Neff and Asner*, 2001] in the soil column influence leaching losses, as these processes represent alternative sinks to hydrological exports.

[30] DON exports are overlooked in most models. Here we treat DOM dynamics in a simple framework taking into account production, buffering and decomposition and leaching. Production of dissolved organic matter (P_{DOM}, in units kgC m^{-2}) is modeled to be proportional to the decomposition of the structural litter and soil water content θ:

$$P_{\mathrm{DOM}} = f_{\mathrm{DOM}}\theta F_{\mathrm{DEC,LS}} \tag{12}$$

where $F_{\mathrm{DEC,LS}}$ is the decomposition flux out LS (Table 1) and f_{DOM} is the fraction which enters the soil DOM pool. In-column DOM decomposition occurs at the rate of slow soil organic matter, and hydrologic losses of DOM (L_{DOM}) are calculated on the basis of drainage rate and a buffer/sorption parameter b_{DOM}, while using the soil volume h_s to convert DOM mass in DOM concentration:

$$L_{\mathrm{DOM}} = \frac{Q_{W,D}}{h_s b_{\mathrm{DOM}}}\mathrm{DOM} \tag{13}$$

where DOM refers to the amount of DOM in the soil column. C and N of DOM are linked by a fixed C:N ratio (r_{DOM}). A more detailed representation of DOM in soils could include vertical transport with sorption-desorption pattern that depends on soil properties, as well as considerations of water flowpaths within the soil column. We feel this simplification is appropriate in light of the sparse knowledge about the specific mechanisms.

2.6. Biological Nitrogen Fixation

[31] Despite its importance to carbon exchange, N fixation is rarely resolved in dynamic land models. When considered, fixation has generally been prescribed on the basis of either reconstructions or scaled to ecosystem properties [*Schimel et al.*, 1997; *Thornton et al.*, 2007]. Symbiotic fixation by plants can bring substantial amounts of new N into ecosystems [*Cleveland et al.*, 1999], whereas fixation by soil heterotrophic bacteria appears to contribute less (1–4 kg N $ha^{-1}yr^{-1}$) in most terrestrial ecosystems [*Crews et al.*, 2000; *Vitousek and Hobbie*, 2000]. Furthermore, BNF is highly variable temporally and spatially: N fixing plant species in temperate and boreal regions (e.g., alders) are few and limited to recently disturbed communities, whereas tropical species (e.g., legumes) are abundant even in mature plant communities [*Crews*, 1999]. New evidence suggests that individual N fixing plants in tropical forests down-regulate their N fixation if sufficient N is available in local environments [*Barron*, 2007]. These observations suggest a biome-scale difference in which the niche for symbiotic N fixation persists in the tropics, but is lost over successional time in temperate/boreal forests. Physiological models have emphasized light requirements and energetic costs of fixation or introduced tradeoffs between plants acquiring N by fixation versus by root uptake [e.g., *Vitousek and Field*, 1999; *Rastetter et al.*, 2001], potentially in combination with the production and activity of phosphatase enzymes [*Wang et al.*, 2007; *Houlton et al.*, 2008].

[32] We consider the inherent differences between tropical and extratropical systems and follow the approach of physiological models that treat N fixation as a costly process with high light requirements, and is therefore only opportune if N demands cannot be met by root uptake [*Rastetter et al.*, 2001]. We do not explicitly distinguish between fixing versus nonfixing species, but rather simulate biological N fixation for the whole community. We define the change of N fixation over time (expressed per unit leaf mass), df_{fix}/dt, as a function of the plant community's potential to adjust its fixation rate to the current N demand (Ψ, see below).

$$\frac{df_{\mathrm{fix}}}{dt} = \lambda_f \frac{\psi}{C_L} - \sigma_f f_{\mathrm{fix}} \tag{14}$$

where λ_f and σ_f are time scales associated with up- and down-regulation of BNF. In extratropical systems, λ_f represents an establishment rate of fixing species, depending on light availability

$$\lambda_{f,\mathrm{extratropic}} = \lambda_{f,0,\mathrm{PFT}} e^{-\tau \mathrm{LAI}} \tag{15}$$

where $\lambda_{f,0,\mathrm{PFT}}$ is an establishment rate without light constraints, τ is the light extinction coefficient, and LAI is the leaf area index. In equation (14), σ_f represents the mortality rate of N fixers for extratropical PFTs.

[33] For the PFT representing tropical forest where N fixing species commonly occupy the canopy, the change in fixation rate is independent of light availability. Thus λ_f collapses to $\lambda_{f,0}$ with $\lambda_{f,0}$ and σ_f representing the time scale of growth and decay of nodules, respectively.

[34] The local demand for N fixation (Ψ) is modeled on the basis of the accruing plant N deficit (D, in units kg N m^{-2} yr^{-1}) and a function κ reflecting N status (x):

$$\psi = D\kappa(x) \tag{16}$$

The N deficit D is the difference in N requirements compared to current total plant intake. D is evaluated on the basis of the daily average for the potential, not N restricted, photosynthesis rate compared to plant N intake:

$$D = \max\left[\frac{NPP_{\mathrm{pot}} - Q_{C,\mathrm{liv}}}{r_{p,\mathrm{target}}} - \left(f_{\mathrm{fix}} C_l + U_{N,P} - Q_{N,\mathrm{liv}}\right), \quad 0\right] \tag{17}$$

where $\mathrm{NPP}_{\mathrm{pot}}$ is the potential NPP if there was no nitrogen restriction, $Q_{C,\mathrm{liv}} = \alpha_l C_l + \alpha_r C_r + \alpha_{\mathrm{sw}} C_{\mathrm{sw}}$ is the combined leaf, root, and sapwood turnover losses (see also equation (2) and Text S3), and $r_{p,\mathrm{target}}$ is the combined living plant C:N ratio including target storage size (equation (3)). In equation (16), κ links the increasing competitive advantage of N fixers to the sensitivity of C assimilation to the plant's N status (x): BNF becomes more opportune, the stronger primary production is scaled down per unit decrease x. Likewise, in tropical trees the tendency toward nodulation increases with decreasing x. We define thus κ in equation (16) to scale to the derivative of equation (4) with respect to x:

$$\kappa(x) = \frac{\phi e^{-\phi x}}{1 - e^{-\varphi}} \tag{18}$$

where the denominator asserts that κ integrated over the range of x (0,1) is 1. A carbon cost associated with BNF is transferred from the plant's living carbon pool (C_{liv}) to LF. Overall we treat BNF as an adaptive and demand driven process with fundamental different adjustment mechanisms between tropics and extratropics.

2.7. Model Forcing and Simulations

[35] We force the model using a combination of output from GFDL's AM2 model and observed precipitation [*GFDL Global Atmospheric Model Development Team*, 2004; *Nijssen et al.*, 2001]. We recycle this data over a horizon of 16 years to perform long-term simulations. In the simulations presented here, we do not address global change scenarios. Therefore we assume preindustrial CO_2 concentrations of 280 ppm and prescribe estimates of preindustrial N deposition [*Dentener and Crutzen*, 1994; *Green et al.*, 2004] as a uniform annual rate. The spatial resolution for global simulations is set to 3.75 degrees longitude times 2.5 degrees latitude.

[36] We analyze the model in three different scenarios: steady state with respect to climate, a step increase in atmospheric CO_2, and a rare but catastrophic local disturbance event. For each scenario, we compare simulations that either include C-N feedbacks or consider only the C model (which assumes unlimited N for the vegetation); this comparison allows us to evaluate the model's behavior relative to the inclusion of C-N feedbacks. The local disturbance experiments consider typical sites in temperate

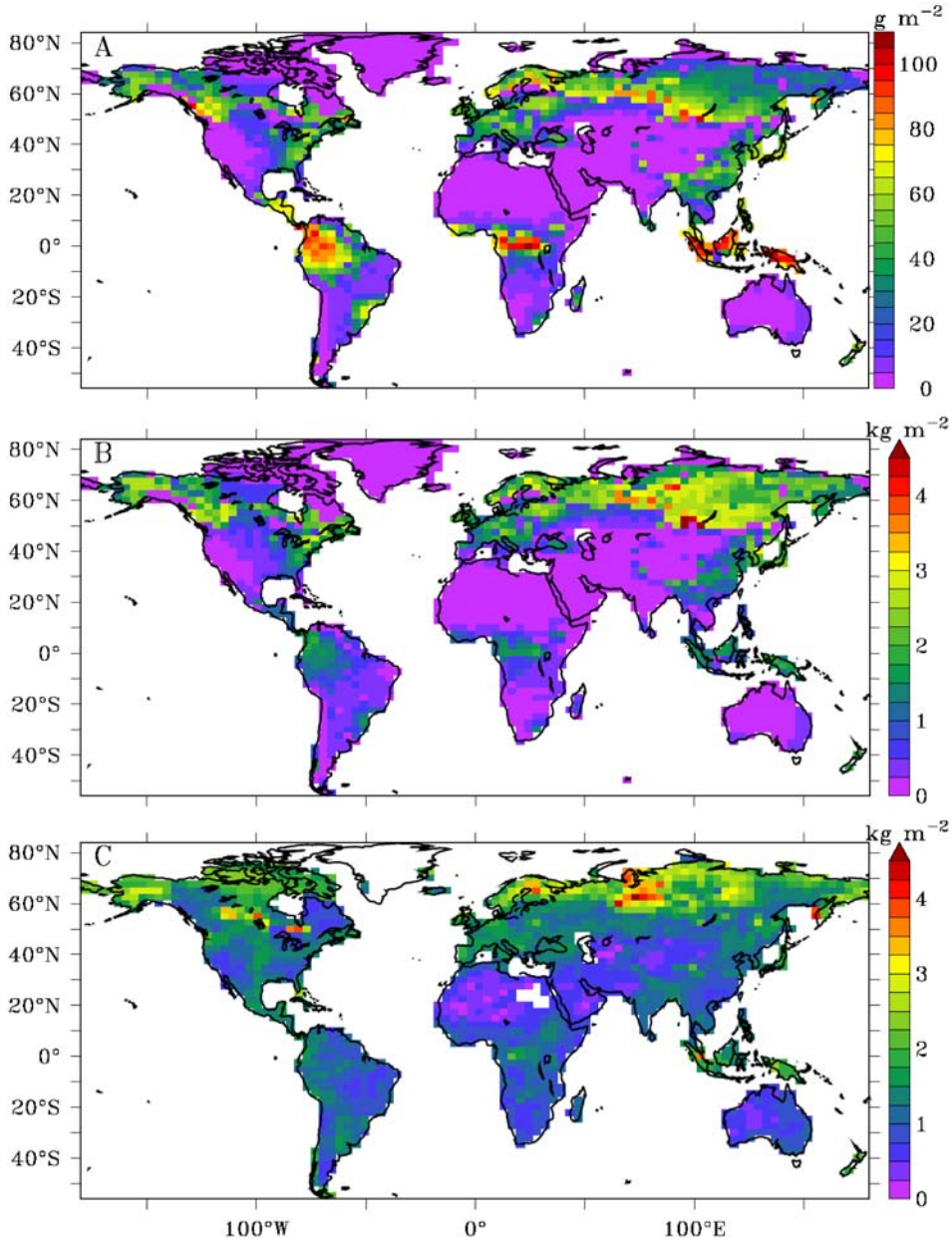

Figure 2. Simulated N in (a) vegetation (live tissues, storage, and wood) and (b) soil (LF + LS + SS + SP). (c) A reconstruction of total soil N [*Global Soil Data Task Group*, 2000].

versus tropical biomes (76°W, 46°N versus 101°W, 0°N). We mimic catastrophic disturbance by removing 95% of vegetation biomass. In addition, we conducted sensitivity experiments in which we sequentially shut off central mechanisms: plant C-N feedback, soil C-N feedbacks, dynamic BNF, and DON losses. We also increased the length of the planning horizon (t_h) to explore effects of the plasticity in vegetation C:N ratio.

[37] The model runs were carried out with the parameter set as provided in Table S1 and Text S2. We accelerated initialization in the first 250 years of integration by equilibrating soil pools every 16 years with the momentary rates of input; afterward, we ran the model for an additional 800 years to reach steady state. To reduce drift, we do not allow the passive soil organic matter pool SP to interact after year 250 (i.e., flux into SP and decomposition of SP are set to zero).

3. Results

[38] At global steady state, our model produces a reasonable estimate of N and C in vegetation and soils (simulation C-N, Figure 2). Simulated global N inventories are close to

Table 2. Biome-Specific N Fluxes and Effects of N on C Fluxes, Vegetation C Inventory, and PFT Distribution[a]

	C4 Grass	C3 Grass	Temperate, Cold Deciduous	Tropical	Cold Evergreen	Total
			N Fluxes (kg ha^{-1} yr^{-1})			
N deposition	0.9	0.6	0.8	1.8	0.4	0.9
Mineralization	79	36	60	81	30	60
N fixation	23	3.8	1.1	2.6	0.7	9.8
DON export	0.1	0.1	0.6	1.1	0.3	0.3
DIN export	13.7	2.3	1.2	3.2	1.0	6.4
Volatile losses	9.8	2.1	0.1	0.1	0.3	4.1
			C-N Feedbacks			
NPP (kgC m^{-2} yr^{-1})						
C-N	0.29	0.16	0.56	0.77	0.25	0.36
C	0.40	0.18	0.59	0.77	0.26	0.41
Vegetation C (kgC m^{-2})						
C-N	0.25	0.19	8.92	13.17	5.27	4.13
C	0.45	0.95	9.26	13.03	5.29	4.40
NEE (kgC m^{-2} yr^{-1})						
C-N	0.007	0.008	0.011	0.052	0.005	0.010
C	0.012	0.010	0.015	0.053	0.005	0.011
Area (10^{12} m^2)						
C-N	53	24	13	25	27	143
C	50	18	19	28	27	143

[a]Steady state values for the coupled C-N and the C-only simulation (C). N fluxes are evaluated for the coupled C-N model. NEE denotes the interannual variability of the net ecosystem change over 96 years, expressed as 1 standard deviation. With the exception of area, the values for the C-only simulation are based on the PFT (i.e., biome) distribution of the C-N realization. Effects of C-N interactions therefore also include shifts in biogeography (e.g., the strong increase in vegetation carbon resulted from forest to grassland conversions when C-N feedbacks are considered).

estimates based on field data reconstructions [*Post et al.*, 1985; *Global Soil Data Task Group*, 2000; *Schlesinger*, 1997]: 120 versus 95–140 GtN for soils and 3.1 versus 3.5 GtN for vegetation. Simulated soil N agrees well with reconstructed inventories in high-productivity regions but tends to underpredict compared to the global reconstructions in low-productivity and low-latitude regions (Figure 2b versus Figure 2c). This discrepancy is a direct result of the model's temperature sensitivity during decomposition, which is higher than suggested by the gradients of the global inventory [*Ise and Moorcroft*, 2006]. The model is less capable of resolving variations in C:N ratios between biomes which are between 10 and 15 in warm zones and 15–20 in cooler regions: mean modeled C:N ratio in soils is 15 with little latitudinal variations.

[39] Inspection of the fluxes of N at steady state reveals a distinct dichotomy in openness of the N cycle as a function of fire frequency (Table 2; N fluxes). On one hand, moist forests are subject to few fires and display high rates of internal N cycling: mineralization and plant uptake range from 30 kg ha^{-1} yr^{-1} in boreal forests to 80 kg ha^{-1} yr^{-1} in tropical forests (mineralization and plant uptake), whereas inputs and losses in forests do not exceed 5 kg ha^{-1} yr^{-1}. In contrast, C4 grasslands in warm climates are subject to high N losses by volatilization and by postfire hydrological leaching. While episodic, the long-term mean of these losses can represent a considerable fraction (up to 40%) of annual N mineralization. In turn, N deficits caused by fire-induced losses select for BNF as a feedback to compensate for the N deficiency.

[40] At steady state, it is perhaps not surprising that the degree of N limitation depends strongly on the openness of the N cycle, i.e., the strength of fire disturbances. Biomes in which fire losses of N are high (e.g., grassland savannas) have the strongest reduction in NPP relative to C-only simulations without N restrictions (Table 2; C-N feedbacks). In areas that are less fire-prone, however, strong N retention in the vegetation soil system allows slow but continuous N buildup to a point where nitrogen no longer or only marginally limits C cycling.

[41] Perturbation of the system by a step increase of 200 ppm CO_2 induces strong C-N interactions (Figure 3). The change in NPP in the following 6 years is considerably dampened in the coupled C-N model. Our model response compares well to actual data from the forest FACE experiments [*Norby et al.*, 2005], in that CO_2 fertilization induces N limitation on NPP in forest plots that have not received nutrient treatments, but increases NPP in plots where N additions have removed the N constraint [*Oren et al.*, 2001]. Overall, the C-N interactions following a sudden CO_2 increase are much stronger than at the model's steady state.

[42] Forest disturbances have long been considered to be critical for nutrient dynamic and nutrient limitation [*Vitousek and Reiners*, 1975; *Bormann and Likens*, 1979]. Here the simulated response to a rare but catastrophic event also caused significant disruptions in C and N cycling. In response, the model produces realistic C-N interactions that broadly follow a similar temporal sequence in both the temperate and tropical forests (Figure 4): mineralization briefly exceeds plant and soil uptake after disturbance, thus inducing a pulse of dissolved inorganic nitrogen (ammonium and nitrate, DIN) loss. In following years, however, N is immobilized by excess litter transferred to soil organic matter and by vegetation recovery. This second phase is thus characterized by low N availability, low DIN export, and up-regulation of BNF. In a third phase, soil N declines, and the associated soil mineralization exceeds plant demand and causes enhanced DIN leaching. The fourth and final phase is defined by stabilization of plant and soil pools. As the system approaches steady state, a small amount of net N accumulation allows for relatively small DIN losses. While

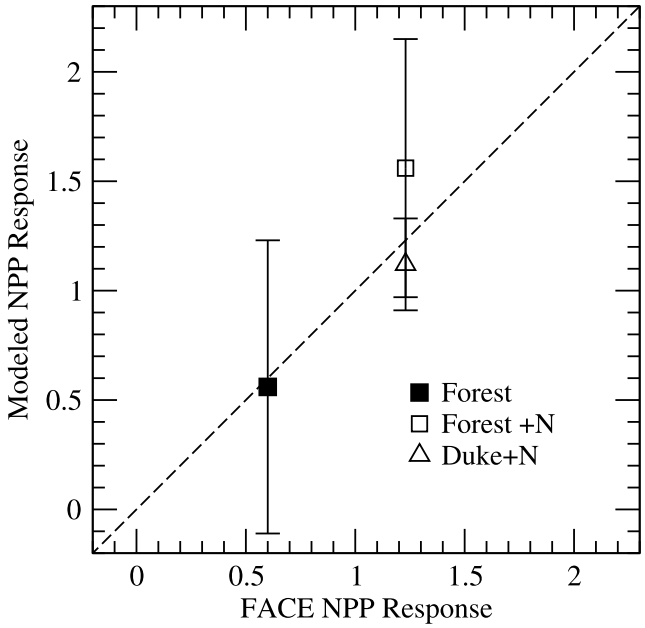

Figure 3. Short-term NPP response of the model to a step change in atmospheric CO_2 by 200 ppm expressed as biotic growth factor (β formulation, $\beta = \frac{NPP_{elev} - NPP_{ctrl}}{NPP_{ctrl}} \log^{-1}\left(\frac{CO2_{elev}}{CO2_{ctrl}}\right)$, where CO_{2elev} and CO_{2ctrl} are the levels of increased and control CO_2 levels, respectively, and NPP_{elev} and NPP_{ctrl} are the NPP at the respective CO_2 levels). The modeled response is evaluated at the locations of the forest free-air CO_2 enrichment (FACE) sites summarized by *Norby et al.* [2005]. The filled rectangle denotes the realization with the coupled C-N model. *Oren et al.* [2001] reported effects of N additions to CO_2 enrichment at the Duke site. We mimicked fertilizer application in the model by shutting off N restriction at the Duke site only (open triangle, Duke+N), and for all FACE sites (Forest+N; note that this result is also compared against the Duke experiment). Vertical bars represent 1 standard deviation of the model's β factor obtained from annual NPP across 6 years and across the different sites.

the temporal sequence of the N pools are qualitatively similar between the temperate versus the tropical site, we also find substantial differences: First, responses in N pools and fluxes were more pronounced in the warmer and more productive tropical forest. For example, postdisturbance leaching was over 5 times greater in the tropical forest. Second, BNF was more pronounced in the tropical forest, with fixation inputs exceeding the temperate BNF by an order of magnitude during the N-poor second phase. Third, recovery and return to steady state is faster in the tropical than the temperate forest; within 300 years the N pools reach their predisturbance levels at the tropical site, compared to a recovery time of almost 1000 years in the temperate forest.

[43] We compared our results against the classical forest watershed disturbance experiment carried out at the Hubbard Brook Experimental Forest [*Bormann and Likens*, 1979]. We performed additional simulations to (1) emulate the herbicide applications used in this experiment, by not permitting plant growth for 3 years following the disturbance and (2) investigate effects of previous wood harvests which occurred earlier at Hubbard Brook Experimental Forest [*Aber et al.*, 2002]. While our simulations could not capture the DIN leaching event that occurred immediately after disturbance, we were able to broadly reconstruct the pattern of N export over the next 30 years. Our inability to capture the early DIN peak might be due to an immediate increase in N immobilization in our model, following the direct incorporation of woody organic matter into the soil environment. In reality, this incorporation may very well have been subject to a delay.

[44] We evaluated the short- and long-term sensitivity of our model to the core feedbacks that we consider in this study: (1) DON losses, (2) N limitation on plant growth, (3) N influence on soil transformations, (4) the physiological planning horizon of plants, and (5) BNF. Disallowing DON losses (thin lines in Figure 4c) causes more rapid accumulation of internal N pools following disturbance and little to no BNF at steady state. The buildup of DIN loss over time indicates that N limitation is not indefinitely maintained in the absence of DON loss. If instead we allow for DON losses (black lines), we find that N limitation persists, which, in turn, causes negligible DIN export and sustained BNF.

[45] We next evaluated the remaining feedbacks by examining their influence on the postdisturbance recovery of C inventories at the tropical and temperate site (Figure 5). Turning off N limitation on either plant growth (mechanism 2, above) or the influence of N on soil C transformations (mechanism 3) had major effects on C dynamics when compared to the baseline model (thick solid line in Figure 5) in which all mechanisms were present. If we simultaneously disallowed both mechanisms (thin solid line), we found that C inventories were substantially elevated following disturbance and that total ecosystem C remained slightly above baseline even once equilibrium was reached. Our results suggests that N effects mediated through plants was greatest immediately following disturbance (when plant growth is rapid but N rare), while the effect mediated through soil transformations occurred over decades to centuries (dashed versus dash-dotted line in Figure 5). Our simulations also showed that the transient N effects on C dynamics were most pronounced in tropical forests, in which plant growth is rapid and thus N demand is greatest.

[46] For tropical forests, we found little difference between a doubling of planning horizon (dotted line in Figure 5) versus baseline in tropical forests. Temperate forests, however, displayed a slightly decreased accumulation of C in the third phase in which N availability is elevated. This is caused by enriched plant N which, in turn, caused less material to flow through the LS-SS pathway (Table 1). In contrast, setting the plant planning horizon to zero (i.e., effectively disallowing N buffering in plants) caused a dramatic decline in ecosystem C pools and recovery after disturbance (results not shown).

[47] Our model was highly sensitive to assumptions about BNF. We replaced our dynamic BNF scheme with

a static fixation rate as identical with the value modeled at steady state (Figure 5, dash-dot-dotted line), corresponding to 3.9 kg ha^{-1} yr^{-1} and 0.5 kg ha^{-1} yr^{-1} for the tropical site for the temperate site, respectively. Static prescribed BNF caused C to dramatically decrease below the baseline model in response to disturbance and greatly slowed down recovery. The response was strongest in the case of tropical forests, in which BNF is critical to maintain high plant growth rates in the face of disturbance.

4. Discussion

[48] We present a model that explicitly couples the terrestrial C and N cycles within the framework of a land

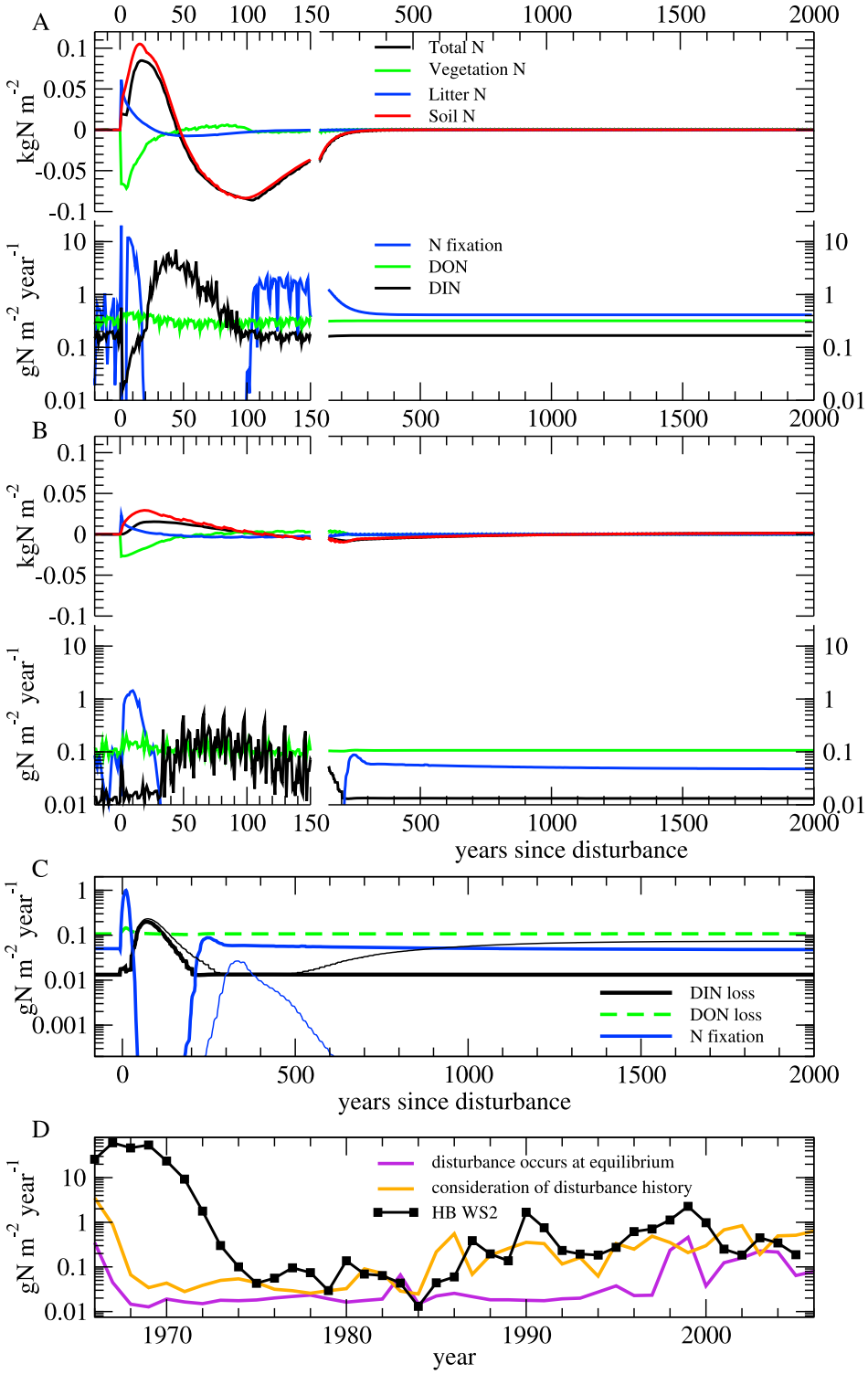

Figure 4

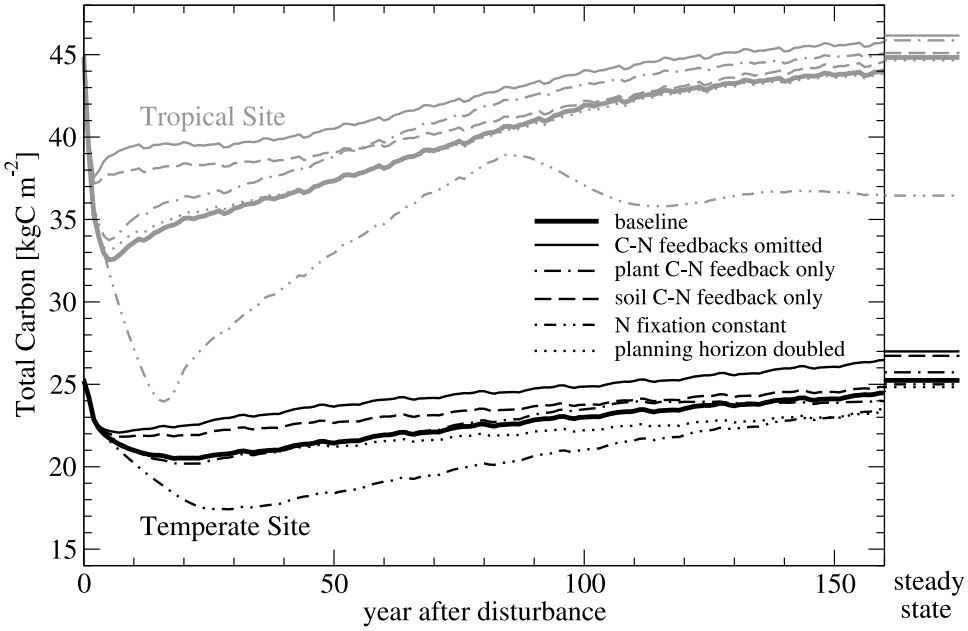

Figure 5. Total terrestrial carbon after the disturbance (Figure 4) for different setups in the N cycle for the tropical (gray) and temperate (black) site. The lines on the right-hand side depict the terrestrial carbon inventory at its steady state 2100 years after the disturbance.

surfaced model (LM3V). By focusing on a set of core mechanisms we address some of the most critical feedbacks between ecosystem N and C cycles. The model combines the capabilities of a land surface model with the current theoretical understanding of N dynamics to resolve key feedbacks between C and N cycling in plants and soils. To our knowledge, the resulting model has one of the most complete representation of biogeochemistry within the complexity and range of a global land surface model. In this evaluation we focus largely on potential vegetation and do not address aspects of humans altering the N cycle (i.e., fertilizer applications and increased N deposition).

[49] We next address our essential processes, one by one, and discuss their impact on ecosystem dynamics, and then return to discuss how these factors interact to generate the resulting patterns shown here.

4.1. Plant N Limitation

[50] Allowing for down-regulation of photosynthesis when plant N reserves are depleted is key for modeling C-N feedbacks. The resulting reduction in ecosystem C is most strongly expressed early in the transient period of postdisturbance recovery (Figure 5). This period is characterized by high N demand from rapid plant growth and low internal supply. We treat plant N limitation in a simple manner: Photosynthesis is adjusted on the basis of plant actual versus optimal N reserves, while the reserves represent an internal buffer that allows plants to accommodate temporary imbalances in N needs compared to C assimilation. In numerical models, plant reserves are often implicitly parameterized, on the basis of prescribed upper and lower limits of tissue C:N ratio, and serve to avoid unrealistic short-term swings between plant N richness and severe limitations. Our model formulation is a conservative approach to prevent this undesired model artifact that might particularly occur when high plant N turnover is combined with too restricted plasticity in tissue C:N ratios. The buffer size appears to be sufficient, because increasing the planning horizon beyond 1 year had little to no effect on overall dynamics. Thus our model offers a reasonable solution for

Figure 4. Response of N pools and fluxes after imposing disturbance where 95% of the vegetation biomass is removed and transferred to the litter pools. The response is shown for (Figures 4a and 4b) a tropical forest site and a temperate forest site. (a) Change in (top) N pools and (bottom) N fluxes at the tropical site shown on two time scales representing initial and long-term consequence of the disturbance. Pools' sizes are shown as deviations from long-term steady state. Fluxes from year 150 on are smoothed with a 16 year running average. (b) Response to disturbance as in Figure 2a at the temperate site. (c) Smoothed fluxes if DON losses are accounted for (thick lines) and set to zero (thin). (d) Comparison of disturbance effects on nitrate losses at the temperate site to the harvest experiment in watershed 2 of the Hubbard Brook Experimental Forest (HB WS2) carried out during the winter of 1965/1966. The model experiment has been modified to prevent growth in the first 3 years after the disturbance. A sensitivity experiment shows the effect of changing initial condition by considering two previous wood harvests in 1870 and 1911 to the disturbance. Wood harvests are approximated with 95% reduction of vegetation biomass where the aboveground fraction of wood and sapwood is assumed to be harvested and the rest of the biomass is transferred to the litter pools.

scaling up physiological mechanisms to the ecosystem level.

4.2. Soil C-N Interactions

[51] Our resolution of belowground C-N interactions follows the traditional approach of CENTURY-type models, which we have amended to include specific C-N feedbacks observed in natural soils: the creation of a pool of N-rich but biologically recalcitrant SOM that often increases with N additions and a sustained up-regulation of decomposition rates in response to N addition. Our analyses and field observations at this point suggest that the net effect of these two processes is relatively small. However, these feedbacks need further evaluation, as they could have profound effects on long-term C-N storage.

4.3. Competing Sinks for Available N

[52] We allow priority of soil/microbial demand over plants which, in turn, outcompete hydrological N losses. Consequently, when soil N immobilization and plant uptake occur at rates below the actual N requirement, available N remains low, and hydrological DIN export is marginal. The negligible export of DIN allows N accumulation over time to the point of N saturation, in particular when DON losses and fire volatilization are also small. The priority of internal demands over exports therefore is a key mechanism that leads to diminishing N limitation as the system approaches steady state.

[53] Currently, the model does not account for denitrification pathways, which could potentially be important in Earth system models, for example, via N_2O emission and radiative forcing feedbacks. While less important for terrestrial C-N feedbacks, a detailed representation of gaseous and hydrological loss pathways of nitrogen becomes necessary to understand the fate of excess nitrogen, particularly for downstream ecosystems (stream, lakes, coastal zones) and for atmospheric chemistry.

4.4. DON Export

[54] Our findings support the idea that DON losses can be an important determinant of the emergence and maintenance of N limitation (Figure 4c): DON losses reduced N accumulation over time and prolonged the recovery of C cycling after disturbance and contributed to sustained N limitation. Despite the importance of DON, however, relatively little is known about how DON losses vary across ecosystems and what factors influence this variation [*McGroddy et al.*, 2008]. Our efforts should therefore be seen as a first step toward a mechanistic representation of DON in global models.

4.5. BNF

[55] BNF is probably the most critical process in the coupled terrestrial biogeochemical cycle, as it is globally the single largest external source of available N and simultaneously extremely heterogeneous in space and time. Yet models apply often either static fixation fields, scale BNF with total ecosystem productivity [*Thornton et al.*, 2007], or evapotranspiration [*Schimel et al.*, 1997]. In our model, static low fixation rate caused declines in C and N pools and induced severe N limitation and slow recovery from disturbance (Figure 5). Conversely, static high fixation rate instead would cause unrealistic N richness which, and in turn, causes misrepresentation of C-N feedbacks and DIN loss patterns. We developed a prognostic formulation that incorporates two essential biological aspects: the dependence of fixation on local N availability and the dependence of fixation on sunlight access in temperate and boreal biomes. As a result, BNF is up-regulated following local disturbances. Therefore an alternative model for extratropical regions could be the parameterization of BNF-based elapsed time since disturbance. For historical simulations, such a succession-based formulation could easily be introduced since LM3V explicitly considers land use transitions.

4.6. Interplay Between Mechanisms

[56] Overall, we found interactions of C and N cycles to be most significant in the transient period that follows disturbance, induced, for example, by logging, windfall, fire, and changes in external forcing (e.g., change in CO_2). However, because of tight internal cycling preventing major DIN losses, N limitation diminishes with time. At steady state we thus find little overall change in net primary productivity (NPP) between simulations that consider C-N feedbacks and those that do not. This is especially true in forested region where we obtain a mere 3% reduction in NPP when C-N feedbacks are accounted for. Particularly, boreal and temperate forests show the most closed N cycle at steady state, with little input from deposition and BNF and concomitant losses that are often dominated by DON. Tropical forests display a moderately closed cycle, where DON and also DIN losses are higher compared to high-latitude forests. The elevated losses are promoted by a higher productivity and a more intense internal cycle, which increase both DON and DIN in soils. N limitation is largely absent in tropical forests because BNF rates adjust quickly to plant N demands.

[57] Over long time scales, we find the most severe N limitation (i.e., reduction in NPP of the coupled C-N simulation versus the C-only model realization) occurred in ecosystems with the most open N cycle. These systems are subject to frequent fire (C4 grasslands) and are those in which the disturbance was associated with significant loss of N. Across different biomes, *LeBauer and Treseder* [2008] found a higher degree of N limitation compared to our model's steady state. However, we show that during transient reorganizations, C-N interactions increase in our model, and the observations may partially reflect disequilibria caused by past human disturbances (clear-cut for pasture and cropland, logging) and current anthropogenic changes (e.g., CO_2 increase).

[58] It is possible that the inclusion of additional nutrients would further improve LM3V: We have designed a model where BNF is a powerful compensatory mechanism that, particularly in the tropics, leads to alleviation of N limitation. Rock-derived nutrients such as phosphorus would adjust less dynamically to limitation. Carrying a prognostic phosphorus cycle could thus be important to capture the full extent of carbon-nutrient feedbacks.

[59] In conclusion, we find strongest feedbacks of N cycling on C cycling where a disruption causes N losses and subsequent limiting effect of N on plant growth, in accordance with current theories on N limitation and suc-

cessional dynamics [*Walker and Syers*, 1976; *Vitousek and Howarth*, 1991]. Thus globally at steady state, fire-prone regions display the strongest susceptibility to N losses and C-N feedbacks. On the other hand, in most forested regions that experience little disturbance, noticeable C-N feedbacks are almost absent on long time scales (steady state). Overall, at steady state, the introduction of equations of N into LMV3 preserves (or alters only little) many features of the C-only model, such as plant productivity, C inventory, and biogeography. These results differ from other models, where great reductions of NPP and C inventories have been found in steady state conditions [*Thornton et al.*, 2007]. However, because of significant C-N interactions during transient reorganizations after perturbations, we expect C-N feedbacks to be of pivotal importance to address the biosphere's role in the current fast-changing climate carbon cycle system.

[60] **Acknowledgments.** We greatly enjoyed discussions with E. N. J. Brookshire, S. Malyshev, H. Levy, S. Bernal, and S. Keel, who helped to improve both the model and this paper. We also thank J. Randerson for a constructive review. Long-term data from Watershed 2 of the Hubbard Brook Experimental Forest were provided by G. E. Likens through support of the National Science Foundation and the Andrew W. Mellon Foundation. This work has been supported by the Cooperative Institute for Climate Science (CICS), NOAA (grant NA17RJ262–344) and NSF award DEB-064166.

References

Aber, J. D., S. V. Ollinger, C. T. Driscoll, G. E. Likens, R. T. Holmes, R. J. Freuder, and C. L. Goodale (2002), Inorganic nitrogen losses from a forested ecosystem in response to physical, chemical, biotic, and climatic perturbations, *Ecosystems*, *5*(7), 648–658.

Barron, A. R. (2007), Patterns and controls of nitrogen fixation in a lowland tropical forest, Panama, Ph.D. diss., 191 pp., Princeton Univ., Princeton, N. J.

Bolker, B. M., S. W. Pacala, and W. J. Parton (1998), Linear analysis of soil decomposition: Insights from the CENTURY model, *Ecol. Appl.*, *8*(2), 425–439, doi:10.1890/1051-0761(1998)008[0425:LAOSDI]2.0.CO;2.

Bormann, F. H., and G. E. Likens (1979), Catastrophic disturbance and the steady state in northern hardwood forests, *Am. Sci.*, *67*, 660–669.

Brooks, P. D., D. M. McKnight, and K. E. Bencala (1999), The relationship between soil heterotrophic activity, soil dissolved organic carbon (DOC) leachate, and catchment-scale doc export in headwater catchments, *Water Resour. Res.*, *35*(6), 1895–1902, doi:10.1029/1998WR900125.

Burns, I., M. Escobar-Gutierrez, and A. Broadley (2001), A role for stomatal conductance in nitrogen-limited growth?, in *Plant Nutrition*, edited by W. J. Horst et al., pp. 104–105, Kluwer, Dordrecht, Netherlands.

Chapin, F. S., E. Schulze, and H. A. Mooney (1990), The ecology and economics of storage in plants, *Annu. Rev. Ecol. Syst.*, *21*, 423–447, doi:10.1146/annurev.es.21.110190.002231.

Cleveland, C. C., et al. (1999), Global patterns of terrestrial biological nitrogen (N2) fixation in natural ecosystems, *Global Biogeochem. Cycles*, *13(2), 623–645, doi:10.1029/1999GB900014.*

Collatz, G., J. Ball, C. Grivet, and J. A. Berry (1991), Physiological and environmental regulation of stomatal conductance, photosynthesis and transpiration: A model that includes a laminar boundary layer, *Agric. For. Meteorol.*, *54*(2–4), 107–136, doi:10.1016/0168-1923(91)90002-8.

Collatz, G., M. Ribas-Carbo, and J. Berry (1992), Coupled photosynthesis-stomatal conductance model for leaves of C4 plants, *Funct. Plant Biol.*, *19*(5), 519–538, doi:10.1071/PP9920519.

Cox, P. M., R. A. Betts, C. D. Jones, S. A. Spall, and I. J. Totterdell (2000), Acceleration of global warming due to carbon-cycle feedbacks in a coupled climate model, *Nature*, *408*(6809), 184–187, doi:10.1038/35041539.

Cramer, W., et al. (2001), Global response of terrestrial ecosystem structure and function to CO_2 and climate change: Results from six dynamic global vegetation models, *Global Change Biol.*, *7*(4), 357–373, doi:10.1046/j.1365-2486.2001.00383.x.

Crews, T. E. (1999), The presence of nitrogen fixing legumes in terrestrial communities: Evolutionary vs ecological considerations, *Biogeochemistry*, *46*(1), 233–246.

Crews, T. E., H. Farrington, and P. M. Vitousek (2000), Changes in asymbiotic, heterotrophic nitrogen fixation on leaf litter of metrosideros polymorpha with long-term ecosystem development in Hawaii, *Ecosystems*, *3*(4), 386–395, doi:10.1007/s100210000034.

Delmas, R., J. P. Lacaux, J. C. Menaut, L. Abbadie, X. Roux, G. Helas, and J. Lobert (1995), Nitrogen compound emission from biomass burning in tropical African savanna FOS/DECAFE 1991 experiment (Lamto, Ivory Coast), *J. Atmos. Chem.*, *22*(1), 175–193, doi:10.1007/BF00708188.

Dentener, F. J., and P. J. Crutzen (1994), A three-dimensional model of the global ammonia cycle, *J. Atmos. Chem.*, *19*(4), 331–369, doi:10.1007/BF00694492.

Downs, M. R., K. J. Nadelhoffer, J. M. Melillo, and J. D. Aber (1996), Immobilization of a ^{15}N-labeled nitrate addition by decomposing forest litter, *Oecologia*, *105*(2), 141–150.

Farquhar, G. D., S. Caemmerer, and J. A. Berry (1980), A biochemical model of photosynthetic CO_2 assimilation in leaves of C3 species, *Planta*, *149*(1), 78–90, doi:10.1007/BF00386231.

Field, C., and H. Mooney (1986), The photosynthesis-nitrogen relationship in wild plants, in *On the Economy of Plants Form and Function*, edited by T. Givinish, pp. 25–55, Cambridge Univ. Press, New York.

Fog, K. (1988), The effect of added nitrogen on the rate of decomposition of organic matter, *Biol. Rev. Camb. Philos. Soc.*, *63*(3), 433–462, doi:10.1111/j.1469-185X.1988.tb00725.x.

Foley, J. A. (1995), An equilibrium model of the terrestrial carbon budget, *Tellus, Ser. B*, *47*, 310–319, doi:10.1034/j.1600-0889.47.issue3.3.x.

Foley, J. A., M. H. Costa, C. Delire, N. Ramankutty, and P. Snyder (2003), Green surprise? How terrestrial ecosystems could affect Earth's climate, *Front. Ecol. Environ*, *1*(1), 38–44.

Friedlingstein, P., et al. (2006), Climate–carbon cycle feedback analysis: Results from the C4MIP model intercomparison, *J. Clim.*, *19*(14), 3337–3353, doi:10.1175/JCLI3800.1.

Galloway, J. N., et al. (2004), Nitrogen cycles: Past, present, and future, *Biogeochemistry*, *70*(2), 153–226, doi:10.1007/s10533-004-0370-0.

Gerber, S., F. Joos, and I. C. Prentice (2004), Sensitivity of a dynamic global vegetation model to climate and atmospheric CO_2, *Global Change Biol.*, *10*(8), 1223–1239, doi:10.1111/j.1529-8817.2003.00807.x.

GFDL Global Atmospheric Model Development Team (2004), The new GFDL global atmosphere and land model AM2–LM2: Evaluation with prescribed SST simulations, *J. Clim.*, *17*(24), 4641–4673, doi:10.1175/JCLI-3223.1.

Global Soil Data Task Group (2000), Global gridded surfaces of selected soil characteristics (IGBP-DIS), data set, Oak Ridge Natl. Lab., Distrib. Act. Arch. Cent., Oak Ridge, Tenn. (Available at http://www.daac.ornl.gov)

Gordon, W. S., and R. B. Jackson (2000), Nutrient concentrations in fine roots, *Ecology*, *81*(1), 275–280.

Green, P. A., C. J. Vörösmarty, M. Meybeck, J. N. Galloway, B. J. Peterson, and E. W. Boyer (2004), Pre-industrial and contemporary fluxes of nitrogen through rivers: A global assessment based on typology, *Biogeochemistry*, *68*(1), 71–105, doi:10.1023/B:BIOG.0000025742.82155.92.

Hedin, L. O., J. J. Armesto, and A. H. Johnson (1995), Patterns of nutrient loss from unpolluted, old-growth temperate forests: Evaluation of biogeochemical theory, *Ecology*, *76*(2), 493–509, doi:10.2307/1941208.

Houlton, B. Z., Y. Wang, P. M. Vitousek, and C. B. Field (2008), A unifying framework for dinitrogen fixation in the terrestrial biosphere, *Nature*, *454*(7202), 327–330, doi:10.1038/nature07028.

Hungate, B. A., J. S. Dukes, M. R. Shaw, Y. Luo, and C. B. Field (2003), Nitrogen and climate change, *Science*, *302*(5650), 1512–1513, doi:10.1126/science.1091390.

IPCC (2007), IPCC fourth assessment report, working group I report, in *The Physical Science Basis*, edited by S. Solomon et al., pp. 501–587, Cambridge Univ. Press, Cambridge, New York.

Ise, T., and P. R. Moorcroft (2006), The global-scale temperature and moisture dependencies of soil organic carbon decomposition: An analysis using a mechanistic decomposition model, *Biogeochemistry*, *80*(3), 217–231, doi:10.1007/s10533-006-9019-5.

Joos, F., et al. (2001), Global warming feedbacks on terrestrial carbon uptake under the intergovernmental panel on climate change (IPCC) emission scenarios, *Global Biogeochem. Cycles*, *15*(4), 891–907, doi:10.1029/2000GB001375.

Knorr, M., S. D. Frey, and P. S. Curtis (2005), Nitrogen additions and litter decomposition: A meta-analysis, *Ecology*, *86*(12), 3252–3257, doi:10.1890/05-0150.

Kucharik, C. J., et al. (2000), Testing the performance of a dynamic global ecosystem model: Water balance, carbon balance, and vegetation structure, *Global Biogeochem. Cycles*, *14*(3), 795–825, doi:10.1029/1999GB001138.

Leadley, P. W., J. F. Reynolds, and F. S. Chapin (1997), A model of nitrogen uptake by Eriophorum Vaginatum roots in the field: Ecological implications, *Ecol. Monogr.*, *67*(1), 1–22.

LeBauer, D. S., and K. K. Treseder (2008), Nitrogen limitation of net primary productivity in terrestrial ecosystems is globally distributed, *Ecology*, *89*(2), 371–379.

Levine, J. (1994), Biomass burning and the production of greenhouse gases, in *Climate Biosphere Interaction: Biogenic Emissions and Environmental Effects of Climate Change*, edited by R. G. Zepp, pp. 139–159, John Wiley, New York.

Li, Y., M. Xu, and X. Zou (2006), Effects of nutrient additions on ecosystem carbon cycle in a Puerto Rican tropical wet forest, *Global Change Biol.*, *12*(2), 284–293, doi:10.1111/j.1365-2486.2005.01096.x.

Lloyd, J., and J. A. Taylor (1994), On the temperature dependence of soil respiration, *Funct. Ecol.*, *8*(3), 315–323, doi:10.2307/2389824.

Matschonat, G., and E. Matzner (1995), Quantification of ammonium sorption in acid forest soils by sorption isotherms, *Plant Soil*, *168–169*(1), 95–101, doi:10.1007/BF00029318.

McGroddy, M. E., T. Daufresne, and L. O. Hedin (2004), Scaling of C:N:P stoichiometry in forests worldwide: Implications of terrestrial Redfield-type ratios, *Ecology*, *85*(9), 2390–2401, doi:10.1890/03-0351.

McGroddy, M. E., W. T. Baisden, and L. O. Hedin (2008), Stoichiometry of hydrological C, N, and P losses across climate and geology: An environmental matrix approach across New Zealand primary forests, *Global Biogeochem. Cycles*, *22*, GB1026, doi:10.1029/2007GB003005.

Melillo, J. M., J. D. Aber, and J. F. Muratore (1982), Nitrogen and lignin control of hardwood leaf litter decomposition dynamics, *Ecology*, *63*(3), 621–626, doi:10.2307/1936780.

Neff, J. C., and G. P. Asner (2001), Dissolved organic carbon in terrestrial ecosystems: Synthesis and a model, *Ecosystems*, *4*(1), 29–48, doi:10.1007/s100210000058.

Neff, J. C., A. R. Townsend, G. Gleixner, S. J. Lehman, J. Turnbull, and W. D. Bowman (2002), Variable effects of nitrogen additions on the stability and turnover of soil carbon, *Nature*, *419*(6910), 915–917, doi:10.1038/nature01136.

Nijssen, B., R. Schnur, and D. P. Lettenmaier (2001), Global retrospective estimation of soil moisture using the variable infiltration capacity land surface model, 1980–93, *J. Clim.*, *14*(8), 1790–1808, doi:10.1175/1520-0442(2001)014<1790:GREOSM>2.0.CO;2.

Norby, R. J., et al. (2005), Forest response to elevated CO_2 is conserved across a broad range of productivity, *Proc. Natl. Acad. Sci. U. S. A.*, *102*(50), 18,052–18,056, doi:10.1073/pnas.0509478102.

Oades, J. (1988), The retention of organic matter in soils, *Biogeochemistry*, *5*(1), 35–70, doi:10.1007/BF02180317.

Oren, R., et al. (2001), Soil fertility limits carbon sequestration by forest ecosystems in a CO_2-enriched atmosphere, *Nature*, *411*(6836), 469–472, doi:10.1038/35078064.

Pacala, S. W., et al. (2001), Consistent land- and atmosphere-based U.S. carbon sink estimates, *Science*, *292*(5525), 2316–2320, doi:10.1126/science.1057320.

Parton, W. J., D. S. Schimel, C. V. Cole, and D. S. Ojima (1987), Analysis of factors controlling soil organic matter levels in great plains grasslands, *Soil Sci. Soc. Am. J.*, *51*(5), 1173–1179.

Parton, W. J., et al. (1993), Observations and modeling of biomass and soil organic matter dynamics for the grassland biome worldwide, *Global Biogeochem. Cycles*, *7*(4), 785–809, doi:10.1029/93GB02042.

Parton, W. J., D. S. Ojima, C. V. Cole, and D. S. Schimel (1994), A general model for soil organic matter dynamics: Sensitivity to litter chemistry, texture and management, in *Quantitative Modeling of Soil Forming Processes: Proceedings of a Symposium Sponsored by Divisions S-5 and S-9 of the Soil Science Society of America in Minneapolis, Minnesota, 2 Nov. 1992*, edited by R. B. Bryant and R. W. Arnold, pp. 147–167, Soil Sci. Soc. Am., Madison, Wisc.

Perakis, S. S., and L. O. Hedin (2001), Fluxes and fates of nitrogen in soil of an unpolluted old-growth temperate forest, southern Chile, *Ecology*, *82*(8), 2245–2260.

Perakis, S. S., and L. O. Hedin (2002), Nitrogen loss from unpolluted South American forests mainly via dissolved organic compounds, *Nature*, *415*(6870), 416–419, doi:10.1038/415416a.

Post, W. M., J. Pastor, P. J. Zinke, and A. G. Stangenberger (1985), Global patterns of soil nitrogen storage, *Nature*, *317*(6038), 613–616, doi:10.1038/317613a0.

Qualls, R. G., and B. L. Haines (1992), Biodegradability of dissolved organic matter in forest throughfall, soil solution, and stream water, *Soil Sci. Soc. Am. J.*, *56*(2), 578–586.

Raich, J. W., et al. (1991), Potential net primary productivity in South America: Application of a global model, *Ecol. Appl.*, *1*(4), 399–429, doi:10.2307/1941899.

Randerson, J., G. van der Werf, L. Giglio, G. Collatz, and P. Kasibhatla (2007), Global fire emissions database, version 2 (GFEDv2.1), Oak Ridge Natl. Lab., Distrib. Act. Arch. Cent., Oak Ridge, Tenn. (Available at http://daac.ornl.gov/)

Rastetter, E. B., G. I. Ågren, and G. R. Shaver (1997), Responses of N-limited ecosystems to increased CO_2: A balanced-nutrition, coupled-element-cycles model, *Ecol. Appl.*, *7*(2), 444–460.

Rastetter, E. B., P. M. Vitousek, C. Field, G. R. Shaver, D. Herbert, and G. I. Ågren (2001), Resource optimization and symbiotic nitrogen fixation, *Ecosystems*, *4*(4), 369–388, doi:10.1007/s10021-001-0018-z.

Rastetter, E. B., S. S. Perakis, G. R. Shaver, and G. I. Ågren (2005), Terrestrial C sequestration at elevated CO_2 and temperature: The role of dissolved organic N loss, *Ecol. Appl.*, *15*(1), 71–86, doi:10.1890/03-5303.

Schimel, D. S., B. H. Braswell, and W. J. Parton (1997), Equilibration of the terrestrial water, nitrogen, and carbon cycles, *Proc. Natl. Acad. Sci. U. S. A.*, *94*(16), 8280–8283, doi:10.1073/pnas.94.16.8280.

Schlesinger, W. H. (1997), *Biogeochemistry. An Analysis of Global Change*, 2nd ed., Academic, San Diego, Calif.

Shevliakova, E., S. W. Pacala, S. Malyshev, G. C. Hurtt, P. C. D. Milly, J. P. Caspersen, L. T. Sentman, J. P. Fisk, C. Wirth, and C. Crevoisier (2009), Carbon cycling under 300 years of land use change: Importance of the secondary vegetation sink, *Global Biogeochem. Cycles*, *23*, GB2022, doi:10.1029/2007GB003176.

Sitch, S., et al. (2003), Evaluation of ecosystem dynamics, plant geography and terrestrial carbon cycling in the LPJ dynamic global vegetation model, *Global Change Biol.*, *9*(2), 161–185, doi:10.1046/j.1365-2486.2003.00569.x.

Sollins, P., G. Spycher, and C. Glassman (1984), Net nitrogen mineralization from light- and heavy-fraction forest soil organic matter, *Soil Biol. Biochem.*, *16*(1), 31–37, doi:10.1016/0038-0717(84)90122-6.

Swanston, C., P. S. Homann, B. A. Caldwell, D. D. Myrold, L. Ganio, and P. Sollins (2004), Long-term effects of elevated nitrogen on forest soil organic matter stability, *Biogeochemistry*, *70*(2), 229–252, doi:10.1023/B:BIOG.0000049341.37579.86.

Thornton, P. E., J.-F. Lamarque, N. A. Rosenbloom, and N. M. Mahowald (2007), Influence of carbon-nitrogen cycle coupling on land model response to CO_2 fertilization and climate variability, *Global Biogeochem. Cycles*, *21*, GB4018, doi:10.1029/2006GB002868.

Throop, H. L., E. A. Holland, W. J. Parton, D. S. Ojima, and C. A. Keough (2004), Effects of nitrogen deposition and insect herbivory on patterns of ecosystem-level carbon and nitrogen dynamics: Results from the CENTURY model, *Global Change Biol.*, *10*(7), 1092–1105, doi:10.1111/j.1529-8817.2003.00791.x.

van der Werf, G. R., J. T. Randerson, L. Giglio, G. J. Collatz, P. S. Kasibhatla, and A. F. Arellano Jr. (2006), Interannual variability in global biomass burning emissions from 1997 to 2004, *Atmos. Chem. Phys.*, *6*(11), 3423–3441.

Vitousek, P. M., and C. B. Field (1999), Ecosystem constraints to symbiotic nitrogen fixers: A simple model and its implications, *Biogeochemistry*, *46*(1/3), 179–202, doi:10.1023/A:1006185020121.

Vitousek, P. M., and S. Hobbie (2000), Heterotrophic nitrogen fixation in decomposing litter: Patterns and regulation, *Ecology*, *81*(9), 2366–2376.

Vitousek, P. M., and R. W. Howarth (1991), Nitrogen limitation on land and at sea: How can it occur?, *Biogeochemistry*, *13*, 87–115, doi:10.1007/BF00002772.

Vitousek, P. M., and W. A. Reiners (1975), Ecosystem succession and nutrient retention: A hypothesis, *BioScience*, *25*(6), 376–381, doi:10.2307/1297148.

Walker, T. W., and J. K. Syers (1976), The fate of phosphorus during pedogenesis, *Geoderma*, *15*(1), 1–19, doi:10.1016/0016-7061(76)90066-5.

Wang, Y., B. Z. Houlton, and C. B. Field (2007), A model of biogeochemical cycles of carbon, nitrogen, and phosphorus including symbiotic nitrogen fixation and phosphatase production, *Global Biogeochem. Cycles*, *21*, GB1018, doi:10.1029/2006GB002797.

Xu-Ri, and I. C. Prentice (2008), Terrestrial nitrogen cycle simulation with a dynamic global vegetation model, *Global Change Biol.*, *14*(8), 1745–1764, doi:10.1111/j.1365-2486.2008.01625.x.

S. Gerber, L. O. Hedin, S. W. Pacala, and E. Shevliakova, Department of Ecology and Evolutionary Biology, Princeton University, Princeton, NJ 08544, USA. (sgerber@princeton.edu)

M. Oppenheimer, Woodrow Wilson School of Public and International Affairs, Princeton University, Princeton, NJ 08544, USA.